Integrating Thermal-Electric Flexibility in Smart Buildings using Grey-Box modelling in a MILP tool

Marius Bagle[1], Benjamin Manrique Delgado[1], Igor Sartori[1], Harald Taxt Walnum[1], Karen Byskov Lindberg[1,2]
[1]SINTEF Community, Oslo, Norway
[2]Norwegian University of Science and Technology (NTNU), Trondheim, Norway

Abstract

In a smart grid setting, building managers are encouraged to adapt their energy operations to real-time market and weather conditions. However, most literature assume stationary temperature set points for heating and cooling. In this work, we propose a grey-box model to investigate how the energy flexibility of the thermal mass of the building may impact its energy flexibility potential as well as the investment decisions of the energy system within a building, by using an already developed investment decision tool, BUILDing's OPTimal operation and energy design model (BUILDopt) (Lindberg et al. (2016)). As BUILDopt is a Mixed Integer Programming (MIP/MILP) tool, the flexibility models must be linear as well. We evaluate the energy flexibility potential, here called *comfort flexibility*, for use cases reflecting different heating systems (electric panel ovens vs. ground source heat pump) and operation (flexible vs. non-flexible). The case study of an Office building is performed, which considers electric specific demand, domestic hot water demand and space heating demand. Real historical data for weather and energy prices from Oslo are used, including grid tariffs related energy and monthly peak power. Most of the savings are obtained through peak load reduction, which can reach up to 13-16%. These and the savings from shifting demand away from peak prices lead to total savings of around 2%. Yet, these actions do not require additional investment in heat supply or storage components, nor in building renovations: only system measurement and control components are needed.

Introduction

The use of the inherent thermal mass in a building is a promising way to enable demand-side response, i.e. controlling a building's energy demand through price signals. While the thermal mass itself comes at no cost, there are costs associated with activating its energy flexibility.

To be able to study the effect of activation of the thermal mass of building as a flexibility resource, the indoor temperature needs to be modelled. To implement this in investment optimization models based on MILP formulations, the model must be linear. The approach of using linear Grey-box models for building envelopes is well established in the domain of Model Predictive Control (MPC) for buildings (Drgoňa et al. (2020)). Grey-box models combine reduced-order models based on simple physics with data-driven inference of the parameters (Bacher and Madsen (2011)). The use of low order representations of building envelopes for investigating flexibility has been demonstrated for district heating systems (Romanchenko et al. (2018)) and energy planning tools (Georges et al. (2021)). A common factor for these approaches is that they use a deviation from a reference temperature instead of the absolute temperature. A direct representation of the indoor temperature with a grey-box RC-network model for energy planning purposes was demonstrated by (Hedegaard et al. (2020)).

According to the IEA Annex 67, energy flexibility of a building is defined as *the ability to manage its demand and generation according to local climate conditions, user needs and grid requirements. Energy flexibility of buildings will thus allow for demand side management or load control and thereby demand response based on the requirements of the surrounding grids* (IEA ECB Annex 67 (2019)). In this paper, we evaluate the impact of *comfort flexibility*, which is the flexibility attained by deviating from normal set-points of the indoor temperature, e.g. by overheating. In this work, we represent this flexibility explicitly with the help of a grey-box model (Bagle et al. (2021)), usually envisioned for usage in an operational control setting. The methods are applied to a case study of an Office building, with given load profiles for electric specific demand, domestic hot water demand and space heating demand (Lindberg et al. (2019)). To enforce consistency between the results (i.e. a cross-comparable baseline case), we create synthetic temperature profiles by forcing the grey-box model to follow the stationary space heating load profile.

Method and model

MILP Model formulation

In the following, we describe the extensions of the MILP BUILDopt model (Lindberg et al. (2016)) which has been re-implemented in the open-source Python-based optimization suite Pyomo (Hart et al. (2017)). BUILDopt is a techno-economic optimisation tool applied to a single building. The model supports investments in heating technologies, storage technologies and power generating technologies. With its hourly time resolution, BUILDopt accounts for detailed operational insights. The objective

function represents the net present value (NPV) of the total costs of the energy system within the building, which depends on the installed capacity, x_i, of each energy technology i. The discounted investment costs, c^{inv}, consist of re-investments throughout the entire lifetime of the building minus its salvage value at the end of the lifetime. c^{run} is the sum of fixed maintenance costs and variable fuel costs. The discounted NPV of the total operational costs equals the annual operational costs divided by the annuity factor, $\epsilon_{n,r}$. The building's energy system must fulfill the equalities $\mathbf{h}(x_i, k_j)$, and inequalities $\mathbf{g}(x_i)$ constraints dependent on the installed capacity for all the energy technologies of the vector **x**.

$$\min \pi = \sum_{i \in \mathcal{I}} c_i^{\text{inv}}(x_i) + c_i^{\text{run}}(x_i, k_j) \tag{1}$$

$$s.t. \mathbf{h}(x_i, k_j) = 0 \tag{2}$$

$$\mathbf{g}(x_i) \geq 0 \tag{3}$$

where x_i is the size of each technology $i \in \mathcal{I}$, and k_j is the consumption of each energy carrier $j \in \mathcal{J}$.

BUILDopt extensions

Separation of heat demand

What drives the BUILDopt model is the demand for energy, originally separated on electricity demand (D^{EL}) and heat demand (D^{HT}) (Lindberg et al. (2016)). In this paper, the demand for heat is further split into space heating demand (D^{SH}) and domestic hot water demand (D^{DHW}), as first introduced in (Bagle (2019)). The following constraints Eq. 4-6 assure that all the demands $\{D^{\text{EL}}, D^{\text{SH}}, D^{\text{DHW}}\}$ are met for all $t \in \mathcal{T}$:

$$D_t^{\text{EL}} = y_t^{\text{imp}} - y_t^{\text{exp}} - \sum_{i \in \mathcal{I}^{\text{SH}}} y_{i,t}^{\text{SH}} - \sum_{i \in \mathcal{I}^{\text{DHW}}} y_{i,t}^{\text{DHW}} + \sum_{i \in \mathcal{I}^{\text{EL}}} y_{i,t}^{\text{EL}} \tag{4}$$

$$D_t^{\text{SH}} = \sum_{i \in \mathcal{I}^{\text{SH}}} q_{i,t}^{\text{SH}} \tag{5}$$

$$D_t^{\text{DHW}} = \sum_{i \in \mathcal{I}^{\text{DHW}}} q_{i,t}^{\text{DHW}} \tag{6}$$

Here, $y_{i,t}$ represents both the generation of electricity from technology $i \in \mathcal{I}^{\text{EL}}$, and the use of electricity in heat technology $i \in \mathcal{I}^{\text{SH}} \cup \mathcal{I}^{\text{DHW}}$. $q_{i,t}$ is heat generated by technology $i \in \mathcal{I}^{\text{SH}} \cup \mathcal{I}^{\text{DHW}}$. Notice that $\mathcal{I} = \mathcal{I}^{\text{SH}} \cup \mathcal{I}^{\text{DHW}} \cup \mathcal{I}^{\text{EL}}$. The internal gains from occupants and electricity demand are not shown in the heat balance, as they are implicitly included in the space heating demand.

Grey-box model representing the space heating demand

A general grey-box model structure for describing the dynamics of the building envelope has been implemented. From (Kristensen and Madsen (2003)), the full model is a stochastic, linear, continuous-time state space model of the form:

$$\dot{z} = \mathbf{A}z + \mathbf{B}u + w \tag{7}$$

where $\mathbf{A}$ is the state transition matrix, $\mathbf{B}$ maps from the inputs $u \in U \subset R^{n_u}$ to the states $z \in Z \subset R^{n_z}$, and $w \in W \subset R^{n_w}$ is the diffusion term. Since we consider deterministic realizations of the models, we assume w to be zero in the discretization, given by (Van Loan (1978)):

$$\mathbf{A}_d = \mathrm{e}^{\mathbf{A}\Delta t} \tag{8}$$

$$\mathbf{B}_d = \mathbf{A}(\mathbf{A}_d - \mathbf{I})\mathbf{B} \tag{9}$$

where Δt is the sampling time, taken to be one hour in this work to make it comply with the rest of BUILDopt. Applying the transformation from continuous-time in Eq. (7) to a discretized state-space given by Eq. (8)–(9), the grey-box model can be implemented directly in BUILDopt using Eq. (10)–(12), $\forall t \in \mathcal{T} \setminus |\mathcal{T}|$:

$$\begin{aligned} z_{t+1}^{\text{l}} =& a_{11} z_t^{\text{l}} + a_{12} z_t^2 + ... + a_{1n} z_t^{\text{n}} + b_{11} u_t^{\text{l}} + \\ & b_{12} u_t^2 + ... + b_{1m} u_t^{\text{m}} \end{aligned} \tag{10}$$

$$\begin{aligned} z_{t+1}^2 =& a_{21} z_t^{\text{l}} + a_{22} z_t^2 + ... + a_{2n} z_t^{\text{n}} + b_{21} u_t^{\text{l}} + \\ & b_{22} u_t^2 + ... + b_{2m} u_t^{\text{m}} \\ & \vdots \end{aligned} \tag{11}$$

$$\begin{aligned} z_{t+1}^n =& a_{n1} z_t^{\text{l}} + a_{n2} z_t^2 + ... + a_{nn} z_t^n + b_{n1} u_t^{\text{l}} + \\ & b_{n2} u_t^2 + ... + b_{mn} u_t^{\text{m}} \end{aligned} \tag{12}$$

where $n = n_x$ and $m = n_u$, and the components of $\mathbf{A}_d$ and $\mathbf{B}_d$ have been written out explicitly. Populating the a's and b's in the grey-box model, we use the results from (Bagle et al. (2021)) and represent the office building as a two-state grey-box model (2R2C), based on data from a white-box IDA-ICE model. Hence, we have a parameterization of the general structure given by Eqs. (10)–(12), with:

$$z_t = [T_t^{\text{in}}, T_t^{\text{e}}]^{\text{T}}, u_t = [\phi_t^{\text{h}}, T_t^{\text{a}}]^{\text{T}} \tag{13}$$

where T_t^{in}, T_t^{e} and T_t^{a}, are the indoor, envelope and ambient temperatures at time step $t \in \mathcal{T}$, respectively. The last step is to replace the input parameter of the space heating demand in BUILDopt, D^{SH}, with the heat consumed by the building ϕ_t^{h}. We rewrite Eq. (5) to:

$$\phi_t^{\text{h}} = \sum_{i \in \mathcal{I}^{\text{SH}}} q_{i,t}^{\text{SH}} \tag{14}$$

By this, the space heat demand is now a variable instead of a parameter. The "comfort"-constraint applied to the envelope model is defined by a lower and an upper bound of the indoor temperature, respectively $T_t^{\text{in,lo}}$ and $T_t^{\text{in,up}}$:

$$T_t^{\text{in,lo}} \leq T_t^{\text{in}} \leq T_t^{\text{in,up}} \tag{15}$$

Case study

This section explains how the data for the reference case is obtained. Then, the case study is described, and we present four different use cases.

Input data

The PROFet model is used to generate load profiles for electric specific demand, space heating demand and domestic hot water demand for an office building with an area of 11,500 m^2, built in accordance to the TEK10 energy efficiency standard in Norway (Direktoratet for byggkvalitet (2016)). The methodology is described in (Lindberg et al. (2019), Andersen et al. (2021)). For the weather (NorskKlimaservicesenter (2021)) and spot price (NordPool (2021)) data, the meteorological year 2012 is used, with Oslo, Norway as the location. D^{EL}, D^{SH} (non-flexible) and D^{DHW} are 2,058 MWh/a, 523 MWh/a and 137 MWh/a, respectively. The grid tariff that is implemented consists of three parts: energy tariff, peak power tariff, and a fixed annual fee. The energy tariff is paid in € per kWh consumed, while the peak power tariff is paid in € per kW monthly peak power. The energy tariff is 0.39 €cent/kWh from April to October and 0.7 €cent/kWh for the rest of the year, while the peak power tariff is 3.6 and 8.5 €/kW for the same periods, respectively. In addition to the aforementioned tariff, the electricity spot price is paid. The NPV of the energy system is calculated for a lifetime of n =60 years, with an interest rate of r =4%.

Calibration efforts to establish the baseline

To establish the baseline for evaluating the flexibility of the building thermal mass, we force the heat generated by the heating technologies, ϕ_t^{h}, to track the stationary profile D^{SH}. That is, we force the heat supply in the model to follow the profile given by PROFet, in order to calculate a proxy temperature. We can formulate an objective function as the minimization of the mean-squared error (MSE) of these two vectors:

$$\min \left(D^{\text{SH}} - \boldsymbol{\phi_t^{\text{h}}}\right)^2 \tag{16}$$

The optimization is performed subject to the constraints in Eq. (10) and (11), where T^{in} is set as a variable, and T^{a} is a parameter. The resulting time series of indoor temperature from this optimization, $T_t^{\text{in,min}}$, is then used as the lower bound for the indoor temperature in Eq. (15). The upper bound, $T_t^{\text{in,up}}$, is calculated as $T_t^{\text{in,min}} + 2°C$. Setting the lower bound temperature this way allows a fair comparison of the greybox-model and PROFet, and gives a conservative estimate of the flexibility potential.

Description of case study

The case study consists of an office building with a total area of 11,500 m^2, assuming that the envelope can be represented by the grey-box model described and identified in Eq. (13). The office building consists of six floors, however, we consider the aggregated dynamics of the building, with T^{in} representing the arithmetic average of the temperature inside the building. We consider two different heating systems, where each system has its own baseline, denoted *nf*, short for *no flexibility*; the activation of the grey-box model for space heating is denoted *flx*. The **DIR** case investigates the flexibility potential if the building is heated with direct electricity using electric panel ovens (*PO*), the most common heating system in Norway (Bøeng, Ann Christin and Halvorsen, Bente and Larsen, Bodil M. (2014)). This configuration falls under the *point-source heating* category, meaning the building does not have a waterborne heat distribution system. The second case, **GSHP**, includes a *waterborne heating system*, heated by a ground-source heat pump (*GSHP*). Both heating systems are complemented by electric boilers (EB) to supply heat to cover D^{DHW}; in the **GSHP** it can also assist during D^{SH} peak loads. In the **DIR** case, the system is limited to PO and EB (only for DHW preparation), and the model can optimize the size of these components. In the **GSHP** case the model can optimize the size of the GSHP and the EB, and it is allowed to invest in storage tanks for domestic hot water and for space heating. The system (component type and size) is calculated in the *nf* case, and the same system is kept for he *flx* case; this allows to focus on the building mass flexibility. The modelling of the hourly COP of the heat pump is based on Standards Norway (2020), combined with several manufacturers' data. Table 1 summarizes the use cases.

Table 1: Case description.

Name	Description
DIR	Building is heated by panel ovens (PO).
GSHP	Building is heated through a waterborne heat distribution system, heated by a ground sourced heat pump (GSHP).
flx	Flexible space heating (activation of thermal mass).
nf	Non-flexible space heating.

Results

In this section, the results of the case studies are presented. Our hypothesis is that by utilizing the building thermal mass, in this paper defined as *comfort flexibility*, a reduction in the space heating cost can be achieved by overheating the building in hours before high prices occur, and by spreading the energy import in order to reduce peak loads. For this, the heat generated by the heat pump or other electric heating must be curtailed or shifted.

Without flexibility

Table 2 shows that the **GSHP** case has the lowest operational costs and lowest amount of electricity bought from the grid. Moreover, the peak load of this system is over 100 kW lower than the **DIR** case. However, the investment costs are over six-fold higher than the **DIR** case that uses electric panel ovens for space heating. The NPV of the total costs is lowest for the case with the ground-source heat pump, however this is without the cost of the waterborne heating distribution system within the building. One way to interpret the difference in NPV between **DIR** and **GSHP**, is as the maximum NPV of the waterborne heating system at which the case **GSHP** is the most profitable. It must be noted that in this investigation, the non-flexible case is still the output of an optimization. Therefore, even

Table 2: Results of selected KPIs.

KPIs	Use Cases			
	DIR		GSHP	
	nf	*flx*	*nf*	*flx*
Peak load [kW]	644	561	537	451
Total cost [k€]	4,254	4,157	3,914	3,840
Cost oper. [k€]	4,191	4,094	3,509	3,436
Cost invest. [k€]	63	63	405	405
El. imp. [MWh/yr]	2,721	2,740	2,319	2,324
Optimal caps.				
Panel ovens [kW]	287.9		-	
GSHP [kW]	-		123.9	
Electric boiler [kW]	26.9		141.3	
SH Tank [kWh]	-		153.7	
DHW Tank [kWh]	-		65.9	

if space heating flexibility is not activated, the model will optimize the operation of the systems components. This becomes notably relevant in the **GSHP** case because of the investments in SH and DHW tanks, as even in the case without flexibility, the model makes optimal use of the storage capacity of the tanks.

Activation of flexibility

Activation of the flexibility reduces the electricity peak load in all cases (cf. Table 2). When activating the thermal flexibility the peak import of electricity is reduced by 13% in the **DIR** case, and by 16% in the **GSHP** case. The reduction of the monthly peak load leads to a subsequent reduction of the peak power tariff. The savings due to this action constitute over 90% of the savings in operation costs in both cases.

Operational details are presented in Fig. 1 and Fig. 2, and are examined more closely in the following.

The figures describing the cases have three plots that show, (from top to bottom) the indoor temperature difference between the *flx* and *nf* cases, heat generated for space heating and electricity imported from the grid. For comparison, the variables of the non-flexible cases *nf* (indoor temperature $T_t^{\text{in,noflex}}$, inflexible heat demand D^{SH} and electricity import $y^{\text{imp,noflex}}$) are included in the second and third plots. Note that y_t^{imp} is the sum of electricity imported for all building loads (see Eq. 4). Hence it can be both smaller and larger than D^{SH}, depending on the coincidence of the loads $\{D^{\text{EL}}, D^{\text{SH}}, D^{\text{DHW}}\}$ and the efficiency of the base load technology.

Fig. 1 shows the operation of the heating system of the **DIR** case in a winter week, with significant spikes in the spot price P^{spot} (grey line) and low outdoor temperatures. The bottom plot shows that the model flattens the peak load and avoids operating the ($q_{PO,t}^{SH}$) when prices are high. The upper plot shows that due to this, the building is often overheated in hours preceding high prices. Since these spikes occur in the morning and evening, a significant part of the overheating must take place at night.

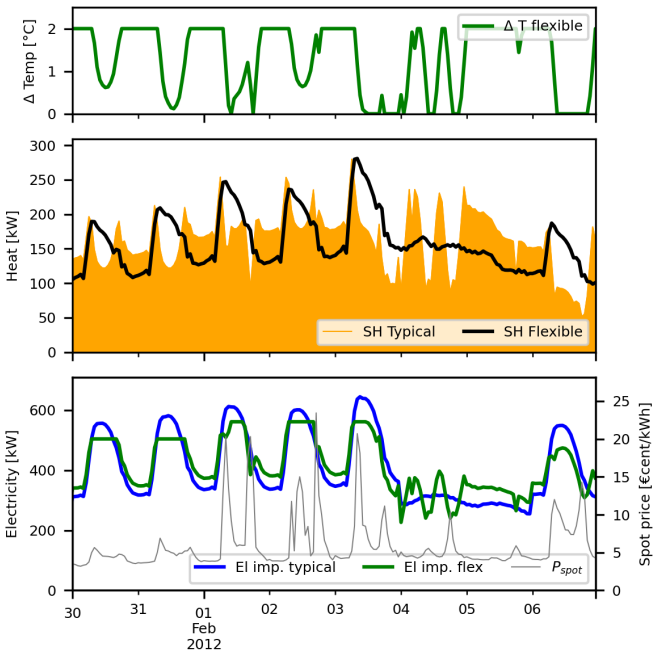

*Figure 1: Operational details of the **DIR-flx** case, week no.5.*

Whether this is acceptable for the end-user is outside the scope of this work. In addition, it is not possible to separate out the bedroom temperature from the aggregate dynamics represented by the average indoor temperature T_t^{in}. It is also noteworthy that the model finds different peak loads for every month, and sets that peak load as maximum import power for every day.

From column **DIR** in Table 2, the annual peak load is reduced by 83 kW, a 13 % decrease, in **DIR**-*flx* compared to **DIR**-*nf*. This is a direct consequence of the power-driven tariff; if this tariff was not considered, the peak load reduction might be lower, and the peak load might even increase. The operational costs are reduced by 97 k€, leading to a 2.3 % reduction in the total cost. The annual imported electricity is increased by $\sim$ 19 MWh/yr compared to **DIR**-*nf*. This quantity corresponds to the losses incurred when storing heat in the thermal mass of the building.

The operation of the **GSHP** case is shown in Fig. 2. A significant difference from the **DIR** case is the presence of a waterborne heating system. Hence, the GSHP and the top-up boiler supply both the space heating (D^{SH}) and domestic hot water (D^{DHW}) demand. However, only D^{SH} is shown in Fig. 2, since the focus of the paper is flexibility from space heating. The tendency towards overheating is similar to the **DIR** case; however, the operation of the GSHP is significantly different to that of the panel oven. The model uses the GSHP nearly constantly at full capacity during the week shown. This is because its COP makes it preferable to the EB, which is only used during hours when the GSHP alone cannot cover the heat demand. The GSHP also supplies heat for DHW demand, which can be seen in the figure as drops in GSHP SH supply during hours when the EB is also operated. Further, the figure

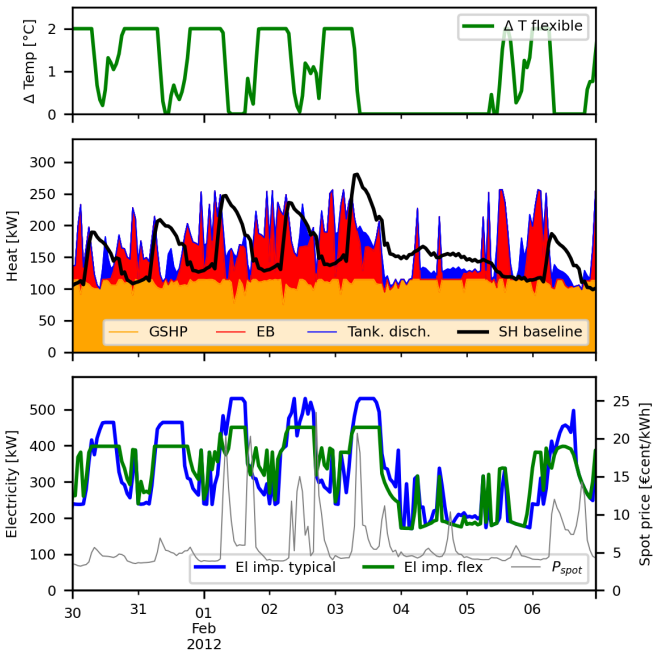

*Figure 2: Operational details of the **GSHP-flx** case, week 5.*

shows how the model uses the SH tank to help keep the indoor temperature within the given limits.

The bottom plots in Fig. 1 and Fig. 2 show remarkably different impact of the EB operation on the imported electricity: while it is mostly absent in Fig. 1, it is significant in Fig. 2. This has two reasons. First, in the **DIR** case the EB is operated exclusively to cover DHW demand, thus having a peak load of only 27.4 kW, whereas in the **GSHP** case it contributes to the SH, and reaches a peak load of 144.2 kW. Second, the peak load of the PO reaches 287.8 kW, whereas the peak load of the GSHP only reaches 44.4 kW. Thus, not only does the EB operate at at five-fold peak power in the **GSHP** than in the **DIR** case, but it also complements a component with roughly one sixth peak import power. The peak load is reduced by ∼86 kW, or 16 %, which is a similar reduction to the **DIR** case, yet the **GSHP** case starts from a lower peak load, as mentioned above.

Discussion

The utilisation of the thermal mass of the building as energy storage allows the model to shift the space heating supply - and thus the electricity import - in a way that reduces the costs incurred through the energy-driven and power-driven tariffs. To implement this action while considering the comfort of the building occupants, this investigation allowed the indoor temperature to be increased by $2°C$ with respect to a baseline temperature. The temperature modulation is in this paper incentivized by the variations of the spot price and the savings from reducing the monthly peak load. It is likely that the cost reductions achieved by the flexibility actions (>73 k€) is large enough to warrant the investment cost of the hardware required for the implementation of a smart control strategy, such as MPC, which can enable demand-side management and hence ”predictive overheating” in a real-time setting. However, most of the savings are obtained through peak load reduction and subsequent savings in the power-driven tariff; if this tariff is not available, which is the case for residential consumers, the savings would be much lower. The power-driven tariff can significantly increase the operation costs. Therefore in some cases, such as during Feb. 3rd. in Fig.2, it is more cost-effective to avoid increasing the peak power than to shift demand away from price peaks, so the optimization model may prioritize peak-shaving instead of shifting loads away from price peaks.

Further, the assumption of ”full”-horizon and perfect knowledge for the operational part of the problem, in the sense that the optimizer sees all disturbances for the whole year with perfect knowledge, makes it optimal to overheat as far ahead as several days before a peak-price event. This might not be feasible in reality, as the increased computational burden entailed by a long prediction horizon would render MPC infeasible in many cases (as most optimal control problems increase ca. cubically in computational complexity with horizon length Drgoňa et al. (2020)). In addition, real-time predictions are not perfect. Moreover, the model is able to find the minimum monthly peak load simultaneously for all days, thus knowing ahead of time what the optimal peak import for the month is. This gives an unrealistic advantage to the model, as in reality the model could only know the peak value of the current and previous days. This could, for example, prevent an MPC from importing at higher power during hours with low prices because it has no knowledge whether the monthly peak will be increased later in the month. Thus, from the practical control perspective, the flexibility potential in this paper is overestimated. However, the baseline is very restrictive. It does not take into account factors such as occupancy, night setback and different thermal zones (e.g. with the indoor temperature being represented by the average, T^{in}). Further, the temperature window is conservatively set at $+2°C$; this delta could be larger, and it may also be negative, thus increasing the window of flexibility. Thus, from a modelling perspective, the flexibility potential might as well be underestimated.

Conclusion

In this paper a grey-box structure has been implemented in a building design optimization tool, BUILDopt, to investigate the flexibility potential of the thermal mass of a building. It has been shown that by utilizing the building thermal mass, in this paper defined as *comfort flexibility*, a reduction in the peak space heating load can be achieved by overheating and thereafter curtailing the heat generated from the peak load technologies. The activation of these flexibility actions leads to modest operational savings of $\sim$ 2%, yet they do not require additional investment in heat supply or storage components, nor in building renovations: only system measurement and control components are needed. Moreover, the monetary impact of the

flexibility actions is closely related to energy prices, so even low percentages could translate to significant savings if prices increase. As well, the energy demand in the building studied here is dominated by the electric specific demand; thus, the flexibility actions may have larger impact in cases where space heating accounts for a higher share of the total energy demand.

It has been shown that the cost of the increased energy consumption due to the flexibility actions can be offset by the savings in the energy-driven and power-driven tariff, with the latter tariff allowing most of the savings. It would thus be of interest to investigate MPC strategies that allow optimal calculation of the monthly peak import with consideration of the limited optimization horizons that are typical in this type of controllers.

Acknowledgment

This paper has been written within the Research Centre on Zero Emission Neighbourhoods in Smart Cities (FME ZEN), grant nr. 257660, and within the research project Flexbuild - "The value of end-use flexibility in the future Norwegian energy system", grant nr. 294920. The authors gratefully acknowledge the support from both the ZEN and Flexbuild partners, as well as the Research Council of Norway.

References

Andersen, K. H., S. K. Lien, H. T. Walnum, K. B. Lindberg, and I. Sartori (2021). Further development and validation of the "PROFet" energy demand load profiles estimator. *Building Simulation 2021 Conference, 1-3 Sep., Bruges, Belgium (BuildSim)*.

Bacher, P. and H. Madsen (2011). Identifying suitable models for the heat dynamics of buildings. *Energy & Buildings 43*, 1511–1522.

Bagle, M. (2019). *Investigation into the impact of thermal energy flexibility on cost optimal design and operation of Zero Emission Buildings*. Master thesis, Department of Electric Power Engineering, NTNU.

Bagle, M. E., P. Maree, H. T. Walnum, and I. Sartori (2021). Identifying grey-box models from archetypes of apartment block buildings. *Building Simulation Conference*.

Bøeng, Ann Christin and Halvorsen, Bente and Larsen, Bodil M. (2014). *"Oppvarming i boliger - Kartlegging av oppvarmingsutstyr og effektiviseringstiltak i husholdningene" Oppdragsrapport for NVE, NVE Report no. 84.*

Direktoratet for byggkvalitet (2016). Byggteknisk forskrift (TEK 10).

Drgoňa, J., J. Arroyo, I. Cupeiro Figueroa, D. Blum, K. Arendt, D. Kim, E. P. Ollé, J. Oravec, M. Wetter, D. L. Vrabie, and L. Helsen (2020). All you need to know about model predictive control for buildings. *Annual Reviews in Control*.

Georges, L., E. Storlien, M. Askeland, and K. B. Lindberg (2021). Development of a data-driven model to characterize the heat storage of the building thermal mass in energy planning tools. *E3S Web of Conferences 246*, 10001.

Hart, W. E., C. D. Laird, J.-P. Watson, D. L. Woodruff, G. A. Hackebeil, B. L. Nicholson, and J. D. Siirola (2017). *Pyomo–optimization modeling in python* (Second ed.), Volume 67. Springer Science & Business Media.

Hedegaard, R., L. Friedrichsen, J. Tougaard, T. Mølbak, Steffen, and Petersen (2020). uSIM2020-Building to Buildings: Urban and Community Energy Modelling, November 12th, 2020, Building Energy Flexibility as an asset in system-wide district heating optimization models.

IEA EBC Annex 67 Energy Flexible Buildings (2019). *Summary report - Energy in Buildings and Communities Programme Annex 67 Energy Flexible Buildings*.

Kristensen, N. R. and H. Madsen (2003). *Continuous time stochastic modelling - Mathematics Guide*. Technical University of Denmark.

Lindberg, K. B., S. J. Bakker, and I. Sartori (2019). Modelling electric and heat load profiles of non-residential buildings for use in long-term aggregate load forecasts. *Utilities Policy 58*, 63–88.

Lindberg, K. B., G. Doorman, D. Fischer, M. Korpås, A. Ånestad, and I. Sartori (2016). Methodology for optimal energy system design of Zero Energy Buildings using mixed-integer linear programming. *Energy and Buildings 127*, 194–205.

NordPool (2021). Historical market data. `https://www.nordpoolgroup.com/historical-market-data/`. (Accessed on 03/18/2021).

NorskKlimaservicesenter (2021). `https://seklima.met.no/observations/`. (Accessed on 03/18/2021).

Romanchenko, D., J. Kensby, M. Odenberger, and F. Johnsson (2018). Thermal energy storage in district heating: Centralised storage vs. storage in thermal inertia of buildings. *Energy Conversion and Management 162*(February), 26–38.

Standards Norway (2020). *Energy performance of buildings — Calculation of energy needs and energy supply (SN-NSPEK 3031:2020)*.

Van Loan, C. (1978). Computing integrals involving the matrix exponential. *IEEE Transactions on Automatic Control 23*(3), 395–404.